AUTHOR QUERY FORM

ELSEVIER	**Journal: ELECOM** **Article Number: 4781**	**Please e-mail or fax your responses and any corrections to:** **Nambiar, Aparna** **E-mail: Corrections.ESCH@elsevier.spitech.com** **Fax: +1 619 699 6721**

Dear Author,

Please check your proof carefully and mark all corrections at the appropriate place in the proof (e.g., by using on-screen annotation in the PDF file) or compile them in a separate list. Note: if you opt to annotate the file with software other than Adobe Reader then please also highlight the appropriate place in the PDF file. To ensure fast publication of your paper please return your corrections within 48 hours.

For correction or revision of any artwork, please consult http://www.elsevier.com/artworkinstructions.

Any queries or remarks that have arisen during the processing of your manuscript are listed below and highlighted by flags in the proof. Click on the 'Q' link to go to the location in the proof.

Location in article	Query / Remark: click on the Q link to go Please insert your reply or correction at the corresponding line in the proof
Q1	Please confirm that given names and surnames have been identified correctly.
Q2	"Institució Catalana de Recerca i Estudis Avançats and Departament de Física" was captured as one affiliation. Please check if appropriate.
Q3	Please check the telephone number of the corresponding author, and correct if necessary.
Q4	"is" was changed to "are" which was assumed to pertain to "conditions". Please check if appropriate.
Q5	Please check if the data found within parentheses are captured correctly and amend as necessary.
Q6	Should "zero-valent" be "zero-valence"? Please check and amend as necessary. Please check this box if you have no corrections to make to the PDF file. ☐

Thank you for your assistance.

Electrochemistry Communications xxx (2013) xxx

Contents lists available at SciVerse ScienceDirect

Electrochemistry Communications

journal homepage: www.elsevier.com/locate/elecom

Graphical abstract

Electrochemistry Communications xxx (2013) xxx–xxx

Anodic formation of self-organized Ti(Nb,Sn) oxide nanotube arrays with tuneable aspect ratio and size distribution

J. Fornell [a,*], N.T.C. Oliveira [b], E. Pellicer [a], N. Van Steenberge [c], M.D. Baró [a], C. Bolfarini [b], J. Sort [d]

[a] *Departament de Física, Universitat Autònoma de Barcelona, 08193 Bellaterra, Spain*
[b] *Department of Materials Engineering – DEMa, Universidade Federal de São Carlos (UFSCar), 13565-905 São Carlos, SP, Brazil*
[c] *OCAS N.V., Pres. J.F. Kennedylaan 3, BE-9060 Zelzate, Belgium*
[d] *Institució Catalana de Recerca i Estudis Avançats and Departament de Física, Universitat Autònoma de Barcelona, 08193 Bellaterra, Spain*

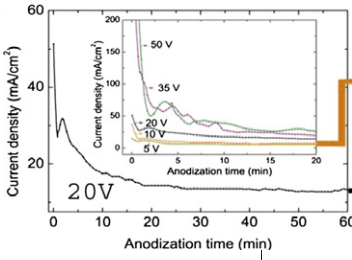

1388-2481/$ – see front matter © 2013 Published by Elsevier B.V.
http://dx.doi.org/10.1016/j.elecom.2013.04.023

Electrochemistry Communications xxx (2013) xxx

Contents lists available at SciVerse ScienceDirect

Electrochemistry Communications

journal homepage: www.elsevier.com/locate/elecom

Highlights

Electrochemistry Communications xxx (2013) xxx–xxx

Anodic formation of self-organized Ti(Nb,Sn) oxide nanotube arrays with tuneable aspect ratio and size distribution

J. Fornell [a,*], N.T.C. Oliveira [b], E. Pellicer [a], N. Van Steenberge [c], M.D. Baró [a], C. Bolfarini [b], J. Sort [d]

[a] Departament de Física, Universitat Autònoma de Barcelona, 08193 Bellaterra, Spain
[b] Department of Materials Engineering — DEMa, Universidade Federal de São Carlos (UFSCar), 13565-905 São Carlos, SP, Brazil
[c] OCAS N.V., Pres. J.F. Kennedylaan 3, BE-9060 Zelzate, Belgium
[d] Institució Catalana de Recerca i Estudis Avançats and Departament de Física, Universitat Autònoma de Barcelona, 08193 Bellaterra, Spain

- One-step anodization is used to prepare self-organized Ti(Nb,Sn) oxide nanotubes.
- Tunable nanoscale geometries can be achieved by varying the anodization conditions.
- The length and the diameter of the NTs tend to increase with the applied voltage.
- Combining TiO_2 with NbO_2 and SnO_2 might provide additional functionalities.

1388-2481/$ – see front matter © 2013 Published by Elsevier B.V.
http://dx.doi.org/10.1016/j.elecom.2013.04.023

Electrochemistry Communications xxx (2013) xxx–xxx

Contents lists available at SciVerse ScienceDirect

Electrochemistry Communications

journal homepage: www.elsevier.com/locate/elecom

Short communication

Anodic formation of self-organized Ti(Nb,Sn) oxide nanotube arrays with tuneable aspect ratio and size distribution

J. Fornell [a,*], N.T.C. Oliveira [b], E. Pellicer [a], N. Van Steenberge [c], M.D. Baró [a], C. Bolfarini [b], J. Sort [d]

[a] Departament de Física, Universitat Autònoma de Barcelona, 08193 Bellaterra, Spain
[b] Department of Materials Engineering — DEMa, Universidade Federal de São Carlos (UFSCar), 13565-905 São Carlos, SP, Brazil
[c] OCAS N.V., Pres. J.F. Kennedylaan 3, BE-9060 Zelzate, Belgium
[d] Institució Catalana de Recerca i Estudis Avançats and Departament de Física, Universitat Autònoma de Barcelona, 08193 Bellaterra, Spain

ARTICLE INFO

Article history:
Received 5 February 2013
Received in revised form 21 April 2013
Accepted 24 April 2013
Available online xxxx

Keywords:
Anodization
Self-organization
Mixed-oxide nanotubes
TiO_2

ABSTRACT

In the present communication one-step anodization is used to prepare large arrays of self-assembled Ti(Nb,Sn) oxide nanotubes on Ti–Nb–Sn alloy. Tuneable nanoscale geometries (unimodal vs. bimodal size distribution with variable length/diameter ratios) can be controllably achieved by varying the anodization conditions, which are highly desirable for enhanced functionalities in widespread applications.

1. Introduction

Bulk TiO_2 is a non-toxic, environmentally friendly and corrosion resistant material. The key functional features are mainly given by its exceptional biocompatibility and the almost unique ionic and electronic properties of this oxide. TiO_2 is a wide band gap semiconductor ($E_g \approx 3$ eV) with suitable band-edge positions that enable its use in solar cells, photocatalysis, electrochromic applications, biomedical coatings, sensors or smart-surface coatings [1]. To improve TiO_2 properties, investigations in this field have been directed towards the development of 1D TiO_2 nanostructures with the aim of increasing the specific surface area (which is crucial for any catalytic reaction) as well as modulating its electronics [1]. Hitherto, the introduction of secondary electronically active species into the lattice of nanostructured TiO_2 has been pursued in order to broaden its range of applications. Among them, niobium and tin species emerge as suitable candidates to dope TiO_2 in order to boost its physiochemical properties.

In the present work, the feasibility of fabricating self-organized nanotubes (NTs) by anodization on Ti–21Nb–11Sn (wt.%) alloy is investigated. Applied voltages have been varied between 5 and 50 V, whereas anodization time has been kept at 1 h. The growth parameters that lead to NTs with controlled diameters and thickness are discussed. It is interesting to mention that the composition of the alloy anodized in this study could possibly provide a material with good biocompatibility, high strength and low Young's modulus, thus minimizing the so-called stress shielding effects [2]. Moreover, since Sn and Nb are less expensive than Ti, the base Ti–Nb–Sn material is inherently less costly than high-purity Ti. To the best of our knowledge, while the growth of an anodic oxide at the surface of Ti–Nb–Sn alloy has already been described [3], the formation of NT arrays has not yet been reported. Furthermore, bearing in mind the synergies achieved upon combining Nb_2O_5 or SnO_2 with TiO_2 NTs, the here-synthesized Ti(Nb,Sn) oxide NTs on the Ti–Nb–Sn alloy will likely enhance the functionality of this material for a wide range of applications.

2. Experimental details

Rods of 4 mm of Ti–21Nb–11Sn alloy (wt.%) were prepared by levitation melting and subsequent injection into Cu mold. Self-organized nanotube oxide layers were grown by electrochemical anodization in 0.31 M NaF + ethylene glycol/water (50:50) electrolyte solution at voltages ranging from 5 to 50 V. Prior to anodization disks of 0.5 mm thick were cut from the rod and ground wet with 1200 grid SiC paper. After anodization, the samples were rinsed for 5 min with ethanol and distilled water in ultrasonic bath and dried at room temperature. To structurally characterize the as-anodized samples Scanning Electron Microscopy (SEM, Zeiss Merlin and Fei Inspect S50), and Transmission Electron Microscopy (TEM, JEOL-2011 200 kV) observations were carried out. X-ray photoelectron spectroscopy (XPS) analyses were conducted on a PHI equipment 5500 Multi Technique using the Al Kα radiation (1486.6 eV).

* Corresponding author. Tel.: +34 935 811 401.
E-mail address: Jordina.fornell@uab.cat (J. Fornell).

1388-2481/$ – see front matter © 2013 Published by Elsevier B.V.
http://dx.doi.org/10.1016/j.elecom.2013.04.023

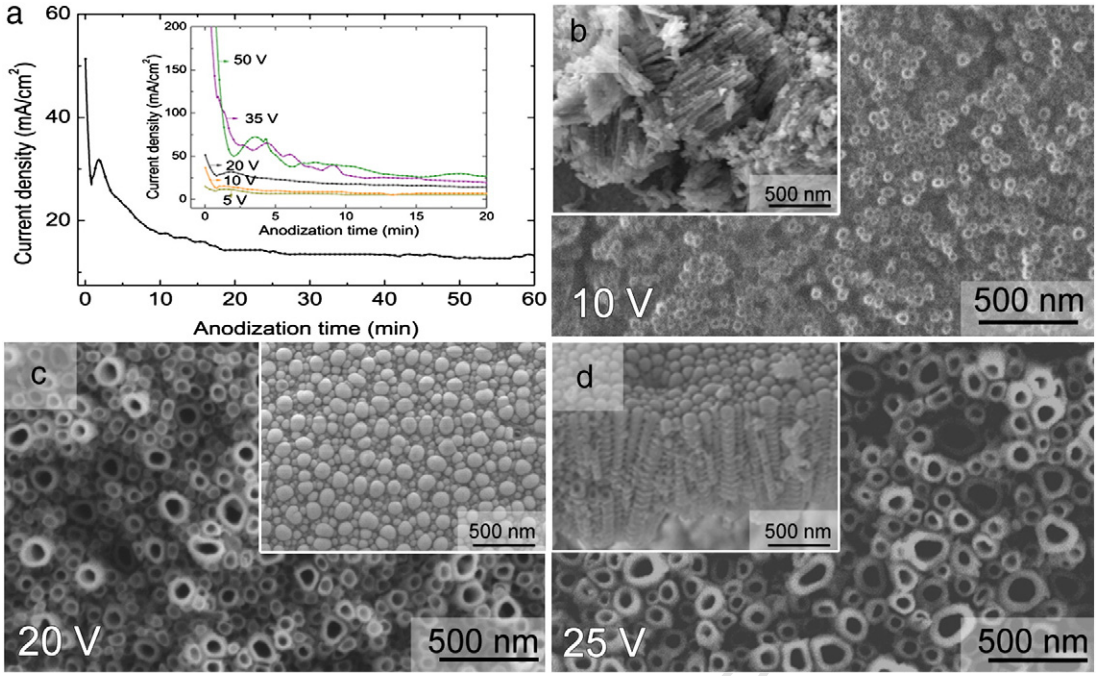

Fig. 1. (a) Current density–anodization time (j–t) curve for the Ti–21Nb–11Sn alloy anodized at 20 V (Inset: j–t curve anodized at 5, 10, 20, 35 and 50 V). (b–d) top view SEM images of Ti–21Nb–11Sn alloy anodized at (b) 10 V, (c) 20 V and (d) 25 V. Insets in (b) and (d) show cross-section-views, while inset in (c) is a bottom view.

3. Results and discussion

Fig. 1a displays the current density–time (j–t) curve recorded during anodization at an applied voltage of 20 V. The curve shows the typical shape for a self-organization process; that is, after an initial exponential decay ascribed to the formation of a compact oxide layer, the current increases until it reaches a maximum value. At this point, the surface is locally activated and pores start growing randomly. Due to the pore growth, the active area increases also resulting in an increase in j. Hereafter, since the pores start interfering with each other, the current density decreases until it reaches a steady-state value (around 13 mA/cm^2) and a self-ordered structure continues growing with time [1,4]. Inset of Fig. 1a displays the j–t curves applied at 5, 10, 20, 35 and 50 V. From these curves, larger current decays are observed as larger potentials are applied. As a result, thicker oxide layers grow at higher applied voltages resulting in larger NT. The curves recorded at 5 and 10 V reach the steady-state value much sooner (after 5 min of anodization) than the others suggesting that, under these conditions, a uniform and continuous nanotubular growth should take place. This observation is in agreement with SEM images of the sample produced at 10 V (Fig. 1b). When the applied voltage is 5 V, however, the nanotube morphology is not well-defined. On the other hand, for an applied voltage larger than 30 V, internal stresses result in NT detachment from the surface during the cleaning process following anodization.

Fig. 1b–d shows SEM images of the structures formed upon anodization of Ti–Nb–Sn alloy at 10, 20 and 25 V. After 1 h of anodization at 10 V, unimodal size distribution is observed (Fig. 1b) whereas

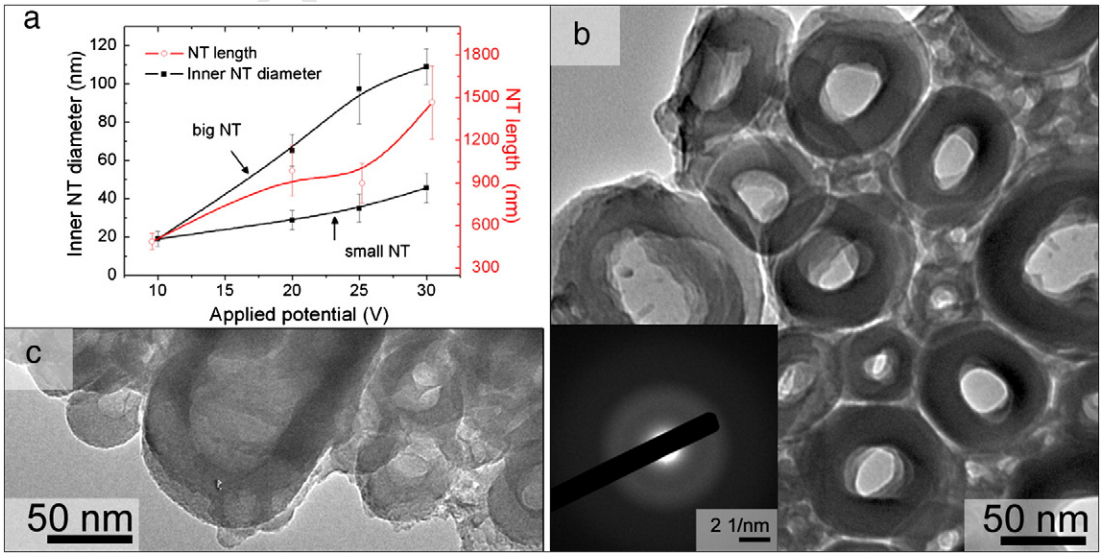

Fig. 2. (a) Dependence of diameter and nanotube length on applied potential, (b–c) TEM microphotographs of nanotubes formed on Ti–21Nb–11Sn alloy, (b) top view image (the inset shows corresponding SAED pattern), (c) cross-section image.

Please cite this article as: J. Fornell, et al., Anodic formation of self-organized Ti(Nb,Sn) oxide nanotube arrays with tuneable aspect ratio and size distribution, Electrochemistry Communications (2013), http://dx.doi.org/10.1016/j.elecom.2013.04.023

Table 1
Elemental composition of the nanotube oxide layer formed at an applied potential of 20 V, determined by XPS, at three different penetration depths (after sputtering with Ar ions for 1, 30 and 60 min).

Element (at.%)		Ti	Nb	Sn	O	F
Sputtering time	1 min	22.9	6.2	1.4	62.2	7.3
	30 min	26.3	8.4	1.6	57.3	6.4
	60 min	27.6	8.9	2	55.3	6.2

bimodal size distribution is detected at larger applied potentials (Fig. 1c and d) where the big NTs are surrounded by the small ones. This bimodal size distribution is even more evident from the bottom view depicted in the inset of Fig. 1c. Here, arrangements consisting of rounded grains of about 120 nm and 48 nm in diameter are seen. The dependence of both the NT diameter and length against the anodization potential is plotted in Fig. 2a. It is interesting to notice that from the test carried out at 10 V, an approximately 500 nm-thick layer of unimodal-sized NTs with a diameter around 20 nm is formed (Fig. 1b). However, inner NT diameters as well as NT length tend to increase with the applied voltage until reaching a 1.7 μm-thick layer of bimodal-sized NTs with diameter sizes around 110 nm and 40 nm for the big and small NTs, respectively, when the applied potential is 30 V. At the intermediate applied potentials, self-organized NT layers were formed consisting of arrays with two distinctly different tube diameters, e.g. of about 67 nm and 30 nm for the alloy anodized at 20 V. Such bimodal size distribution may be attributed to two factors: i) alloy composition (i.e., alloying elements (Nb and Sn) influence the alloy's microstructure and consequently NT growth) and ii) geometry stabilization effects under certain anodization conditions. On the one hand, Ti–21Nb–11Sn is a two-phase material (β and ω phases coexist) that can hinder the growth of uniformly sized NTs. On the other hand, it has been reported that some binary TiX (X = Nb, Zr) alloys show self-organization on two-size scales [5,6], so that the growth factor of the big diameter NTs typically corresponds to that of Ti ($f_{g,TiO_2} \approx 2.5$ nm/V) while that of the small diameter NTs is smaller and, as a consequence, they grow recessed. In our case, f_g would be around 1.6 nm/V for the big NTs and 0.55 nm/V for the small ones.

Fig. 2 shows top view (Fig. 2b) and cross-section (Fig. 2c) TEM images of the structures formed by anodization of the Ti–21Nb–11Sn alloy at 20 V. The TEM images confirm that hollow NT structures with a bimodal size distribution are obtained. Namely, large-diameter NTs with 23 nm-thick walls (big NT) can be observed along with NTs of smaller diameter with 11 nm-thick walls (small NT). No significant differences in composition were observed depending on the NT diameter, at least within the accuracy of the EDX technique. From the Selected Area Electron Diffraction (SAED) pattern (inset of Fig. 2b) the amorphous character of the as-grown NTs is evidenced. In order to evaluate the chemical composition along the tubes, XPS analyses were carried out on the sample produced at an applied voltage of 20 V at three penetration depths. i.e. after sputtering the NT layer with Ar ions for 1, 30 and 60 min. Assuming an etching rate of 5–10 nm min^{-1}, this would give a penetration of 5–10 nm, 150–300 nm and 300–600 nm, respectively [7]. In all cases, the survey spectra indicate the presence of Ti, Nb, Sn, O and F elements, the latter coming from the electrolyte. Quantitative evaluation of the results is shown in Table 1. After sputtering for 60 min an increase of the content of valve elements is detected while the O content slightly decreases, as the measurement is likely

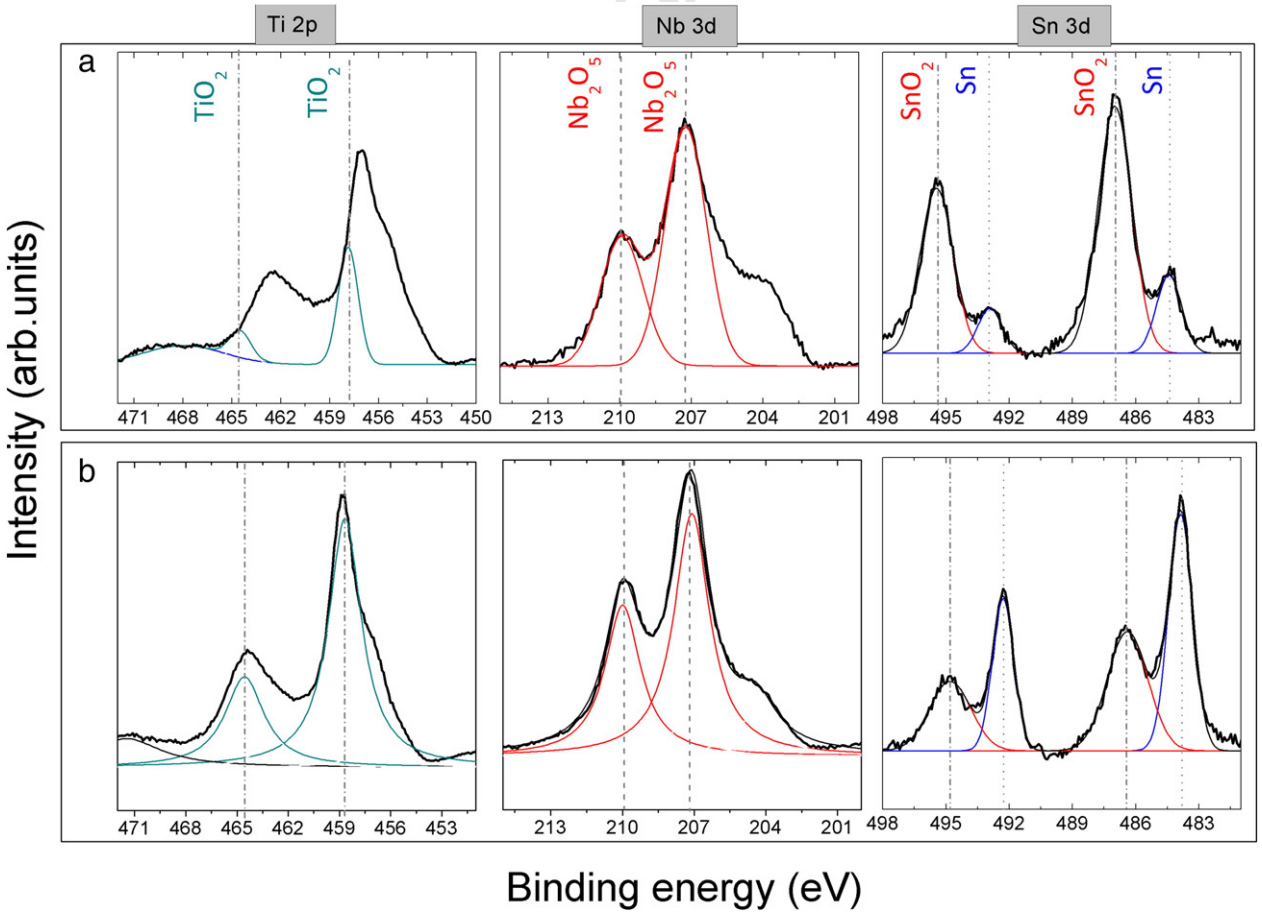

Fig. 3. Ti 2p, Nb 3d and Sn 3d core-level XPS spectra of the nanotube oxide layer formed at an anodizing voltage of 20 V after sputtering with Ar ions for (a) 1 min and (b) 1 min after air-annealing at 923 K for 60 min.

Please cite this article as: J. Fornell, et al., Anodic formation of self-organized Ti(Nb,Sn) oxide nanotube arrays with tuneable aspect ratio and size distribution, Electrochemistry Communications (2013), http://dx.doi.org/10.1016/j.elecom.2013.04.023

performed near the substrate. Ti (arising from TiO_2) is the most abundant element, in agreement with the bulk alloy composition. A detail of the Ti 2p, Nb 3d and Sn 3d regions at t = 1 min is shown in Fig. 3. Multipeak fitting was carried out assuming a Gaussian distribution. The peaks located at 464.6 eV (Ti $2p_{1/2}$) and 458.7 eV (Ti $2p_{3/2}$) are associated with Ti^{4+} valence state [8–10]. Discrepancies between the experimental data and the fitting are probably attributed to the existence of oxygen vacancies. The binding energies of 210.0 eV (Nb $3d_{3/2}$) and 207.2 eV (Nb $3d_{5/2}$) belong to Nb^{5+} [11,12]. Deeper inside (t = 60 min), the zero-valent state of Nb emerges and a decrease of the peaks related to Nb_2O_5 is observed (not shown). Likewise, in the case of Sn, the main peaks at 486.9 eV and 495.4 eV match the Sn^{2+} valence state [11], whereas deeper inside of the nanotubes the main contribution comes from zero-valent state of Sn.

According to the XPS data, the formation of the composite NTs would mainly proceed via the following reactions:

$$2Ti + 2H_2O \rightarrow TiO_2 + 4H^+ + 4e^- \quad (1)$$

$$TiO_2 + 4H^+ + 6F^- \rightarrow [TiF_6]^{2-} + 2H_2O \quad (2)$$

for Ti;

$$Nb + 5H_2O \rightarrow Nb_2O_5 + 10H^+ + 10e^- \quad (3)$$

$$Nb_2O_5 + 10H^+ + 12F^- \rightarrow 2[NbF_6]^- + 5H_2O \quad (4)$$

for Nb;

$$Sn + 2H_2O \rightarrow SnO_2 + 4H^+ + 4e^- \quad (5)$$

$$SnO_2 + 4H^+ + 6F^- \rightarrow [SnF_6]^{2-} + 2H_2O \quad (6)$$

for Sn.

According to several authors TiO_2 anatase could be obtained from the amorphous oxides directly by thermal annealing in air [13,14]. It is interesting to note that TiO_2 anatase nanotubes are believed to possess the highest biocompatibility among other titanium oxides and phases [15]. In our case, after annealing at 923 K for 60 min, α and β-Ti phases (arising from the substrate) and anatase and rutile phases coming from TiO_2 were identified. Detailed XPS analyses of the NT layer indicate that the main compounds resulting from the annealing process are TiO_2, Nb_2O_5 and SnO_2 (Fig. 3c). Niobium and tin oxide films have been previously evaluated in terms of cell growth and wettability with good results [16,17].

4. Conclusions

In summary, the formation of large arrays of self-ordered titanium–niobium–tin mixed oxide nanotubes by a simple step electrochemical self-assembly process is reported. By varying the applied voltage during anodization, the size distribution of the NTs evolves from unimodal to bimodal. Both the length and the inner diameter of the NTs tend to progressively increase with the applied voltage. The precise control of the alloy surface morphology (i.e., NT arrangement geometry) may facilitate and enhance the use of this material in widespread technological applications, including biomedical, photocatalysis, opto-electronic and electrochromic devices or sensors.

Acknowledgments

This work has been supported by the MAT2011-27380-C02-01 and CNPq – Brazil (proc. 150651/2011-2) projects. MDB acknowledges the ICREA-Academia Award.

References

[1] P. Roy, S. Berger, P. Schmuki, Angewandte Chemie International Edition 50 (2011) 2904.
[2] K. Miura, N. Yamada, S. Hanada, T.K. Jung, E. Itoi, Acta Biomaterialia 7 (2011) 2320.
[3] N. Masahashi, Y. Mizukoshi, S. Semboshi, N. Ohtsu, T.K. Jung, S. Hanada, Thin Solid Films 519 (2010) 276.
[4] A. Ghicov, P. Schmuki, Chemical Communications (2009) 2791.
[5] S.-H. Jang, H.-Ch. Choe, Y.-M. Ko, W.A. Brantley, Thin Solid Films 517 (2009) 5038.
[6] J.M. Macak, H. Tsuchiya, A. Ghicov, K. Yasuda, R. Hahn, S. Bauer, P. Schmuki, Current Opinion in Solid State and Materials Science 11 (2007) 3.
[7] X. Batlle, B.J. Hattink, A. Labarta, J.J. Akerman, R. Escudero, I.K. Schuller, Journal of Applied Physics 91 (2002) 1016.
[8] M.C. Biesinger, L.W.M. Lau, A.R. Gerson, R.St.C. Smart, Applied Surface Science 257 (2010) 887.
[9] Y.-L. Chung, D.-S. Gan, k.-I. Ou, S.-Y. Chiou, Journal of the Electrochemical Society 158 (2011) C319.
[10] R. Narayanan, S.K. Seshadri, Journal of Applied Electrochemistry 36 (2006) 475.
[11] J.F. Moulder, W.F. Stickle, P.E. Sobol, K. Bomben, in: J. Chastain (Ed.), Handbook of X-ray Photoelectron Spectroscopy, Second ed., Perkin-Elmer Corporation (Physical Electronics), Eden Prairie, 1992.
[12] A. Mozalev, M. Sakaire, I. Saeki, H. Takahashi, Electrochimica Acta 48 (2003) 3155.
[13] Y.-L. Chung, D.-S. Gan, K.-L. Ou, Journal of the Electrochemical Society 459 (2012) C133.
[14] C.M. Lin, S.K. Yen, Materials Science and Engineering: C 26 (2006) 54.
[15] M. Uchida, H.-M. Kim, T. Kokubo, S. Fujibayashi, T. Nakamura, Journal of Biomedical Materials Research 64A (2003) 164.
[16] E. Eisenbarth, D. Velten, M. Müller, R. Thull, J. Breme, Journal of Biomedical Materials Research. Part A 79 (2006) 165.
[17] N. Rushe, M. Ball, W.M. Carroll, S. Healy, J. McManus, D. Cunningham, Journal of Materials Science. Materials in Medicine 16 (2005) 247.

Please cite this article as: J. Fornell, et al., Anodic formation of self-organized Ti(Nb,Sn) oxide nanotube arrays with tuneable aspect ratio and size distribution, Electrochemistry Communications (2013), http://dx.doi.org/10.1016/j.elecom.2013.04.023